Communications in Physics, Vol. 28, No. 1 (2018), pp. 87-96
DOI:10.15625/0868-3166/28/1/11036

EFFECT OF TiO_2 ANATASE NANOCRYSTALLITE ON ELECTRICAL PROPERTIES OF PPY/TiO_2 NANOCOMPOSITE

DUONG NGOC HUYEN[1,†], THANH-PHUONG NGUYEN[1] AND NGUYEN TRONG TUNG[1,2]

[1]*School of Engineering Physics, Hanoi University of Science and Technology*
No. 1 Dai Co Viet, Hai Ba Trung, Hanoi, Vietnam

[2]*College of Television Vietnam, Thuong Tin, Hanoi 158500, Viet Nam.*

[†]*E-mail:* huyen.duongngoc@hust.edu.vn

Received 30 December 2017
Accepted for publication 19 January 2018
Published 26 March 2018

Abstract. *Polypyrrole/titanium dioxide nanocomposite (PPy/TiO_2) was synthesized by in-situ chemical polymerization of pyrrole (Py) monomer in colloidal suspension of TiO_2 anatase. TEM images show that TiO_2 anatase nanoparticles with size of around 3–4 nm are randomly imbedded on the surface and inside of PPy grain. The random distribution of TiO_2 anatase nanoparticle in PPy matrix forms variety of carrier barriers on the surface and inside of the materials. As expectation, the charge exchange between oxygen and the PPy affects the carrier barrier's regions and then modify the electrical properties of PPy. Upon exposure to the open air the conductivity of the PPy/TiO_2 nanocomposite exhibits an increase of about 20 folds much larger than that of neat PPy. The enhancement is accounted for the modification of in the surface conductance of PPy/TiO_2 nanocomposite as a combination of the TiO_2 coupling and oxygen interaction.*

Keywords: PPy, TiO_2 anatase, nanocomposite PPy/TiO_2, complex impedance spectrum.

Classification numbers: 81.07.Bc; 78.67.Sc; 81.07.-b .

I. INTRODUCTION

The unique structure of alternative single and double bonds in the linear chain of intrinsic conjugated polymers (CPs) [1,2] has found to be susceptible to the ambient chemical and physical interactions. Consequently, the polymer chain will lose or attract some electrons and then converts to either *p*-type or *n*-type semiconducting. The feature has been used as an effective approach to modify the electrical properties of the materials for possible applications [3, 4]. In addition, the coupling of CPs with active constituents can be used as means to tailor functionalities and

design new materials with desirable characteristics. Beyond a simple combination of its property, the interaction between molecules component in the nanocomposite can bring in new features or synergistic effects.

Amongst of most studied CPs, polypyrrole (PPy) and its derivatives have attracted a great deal of attention because of their high electrical conductivity, good environmental stability, simple synthesis and processing [5] and shown to be promising materials for many applications such as electrical wire, sensors, electrochemical capacitors, electronic devices, [2, 4, 6–8], etc. Due to the relatively low oxidation potential the neutral PPy has found to be easily oxidized (doping) into *p*-doped state [9] and reduced (de-doping) back to the neutral form. As a result, the electrical properties of PPy seem to be easily modified by use of proper reduction/re-oxidation process or combination with suitable components in a nanocomposite [10].

On the other hand, titanium dioxide (TiO_2) is a typical oxide metal and *n*-type semiconductor that exhibits strong electrochemical and photochemical activity [11]. Apart from major application in vanishes, paint, etc., that rely on the brightness and high refractive index of TiO_2,theelectrochemical and photochemical features have enlarged the application of TiO_2 in photocatalyst, solar cells,... [12, 13]. Under normal conditions, TiO_2 crystalline has two main structural morphologies: rutile and anatase which show a difference in crystalline, electronic structure and chemical activity. In term of chemoelectrical, photoelectrical, photochemical properties the TiO_2 anatase shows stronger oxidatively while the rutile exhibits higher refractive index [14]. The coupling of more active TiO_2 anatase with conducting polymers in a nanocomposite has found to improve their unique features [15–18], namely sensitivity, electrical conductivity, electrochemical properties, etc.

Based on these assumptions, in this research an attempt was carried out to investigate the effect of anatase nanocrystallites resulted from thermolysis of $TiCl_4$ in HCl aqueous solution [19–21] on PPy/TiO_2 nanocomposites synthesized by *in-situ* chemical polymerization.

II. EXPERIMENT

Pyrrole (Py) 99.5 % and $TiCl_4$ (Aldrich. Co.), ammonium persulphat (APS, Kanto Chemical Co. Inc.) and titanium chloride $TiCl_4$ (Aldrich. Co.) were used as precursors in the experiment. The PPy/TiO_2 nanocomposite was *in-situ* chemically synthesized as followings: TiO_2 nanostructure materials were firstly prepared by the thermal hydrolysis of a titanium precursor ($TiCl_4$). The synthesis was carried on at low temperature ($\sim 80^{\circ}$C) in acidic aqueous media of 0.1 M HCl as a usual route [19,20]. The resulting TiO_2 nanomaterials were separated into two parts containing anatase nanostructures in the colloidal suspension and rutile nanostructures in the sedimentation. The anatase colloidal suspension then was extracted, dried and then mixed with an aqueous solution of 0.1 M Py and 1.0 M HCl with a given TiO_2/Py ratio. Secondly, by adding drop-by drop the same amount of an aqueous solution consisting of 0.1 M APS (as oxidant) and 1.0 M HCl into the TiO_2/Py mixing solution the polymerization of PPy was ignited. After 1.5 hours of continuously stirring the polymerization was terminated by pouring ethanol into the mixture. The resulting black PPy/TiO_2 nanocomposites formed in the solution were filtered, then was cleaned by distilled water and kept in 1.0 M HCl solution.

The morphology, structure, particle size of the TiO_2 anatase and PPy/TiO_2 nanocomposite were characterized by X-ray diffraction (XRD D8 Advance Bruker) and Transmission Electron Microscope (TEM Jeol JEM1010). The electronic structure of the materials was analyzed by

Raman spectra using LabRAM HR800 (Horiba) with a 632.8nm excitation laser ranging from 100-2339 cm^{-1} at a resolution of 4 cm^{-1}. PPy/TiO_2 layers drop-coated on comb-like Pt electrodes were used as test samples to measure the electrical properties of the materials (its resistance and impedance as a function of TiO_2 content, air pressure and nitrogen N_2). The electrical data were acquired and analyzed by Digital Multimeters (Keithley2220G) and by an impedance analyzer (HP4192A).

III. RESULTS AND DISCUSION

The XRD and Raman spectra show that the TiO_2 extracted from the suspension solution is anatase nanocrystallite. As can be seen from the XRD spectrum in Figure 1a, the strongest peak observed around 25.29◦ is assigned to (101) plane refraction of anatase and the other peaks at 37.80, 48.05, 53.89, and 62.68◦ stand for reflection at (004), (200), (105), and (204) planes, respectively (JCPDS number 00-021-1272). Using Scherrer formula to estimate the particle size, it was found that the anatase mean size is around 4.0 nm.

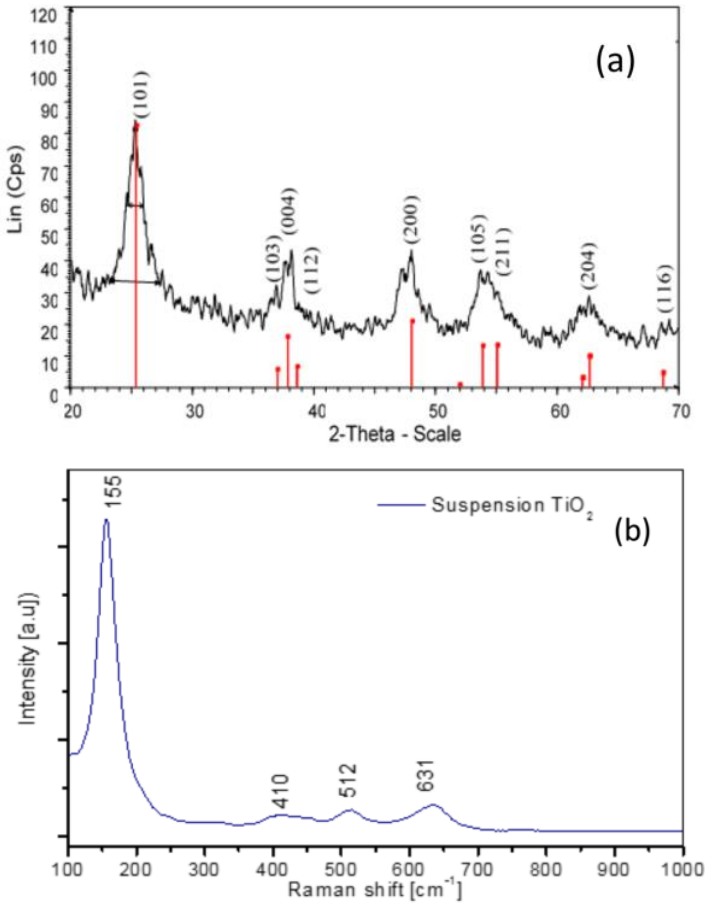

Fig. 1. (a) XRD and (b) Raman spectrum of TiO_2 synthesized by pyrolysis of $TiCl_4$ aqueous solution.

The Raman spectrum of the suspended TiO_2 in Fig. 1b exhibits Raman shift peaks at around 155, 412, 512, and 631 cm^{-1} representing the Eg, $B1g$, $A1g + B1g$, and Eg vibrational modes, respectively of anatase phase [22–24]. In comparison to the standard vibration mode of anatase, the first Eg mode at 155 cm^{-1} shows blue shifts in frequency and increase in width at half maximum that accounts for an influence of the nanosize of the TiO_2 anatase crystallites.

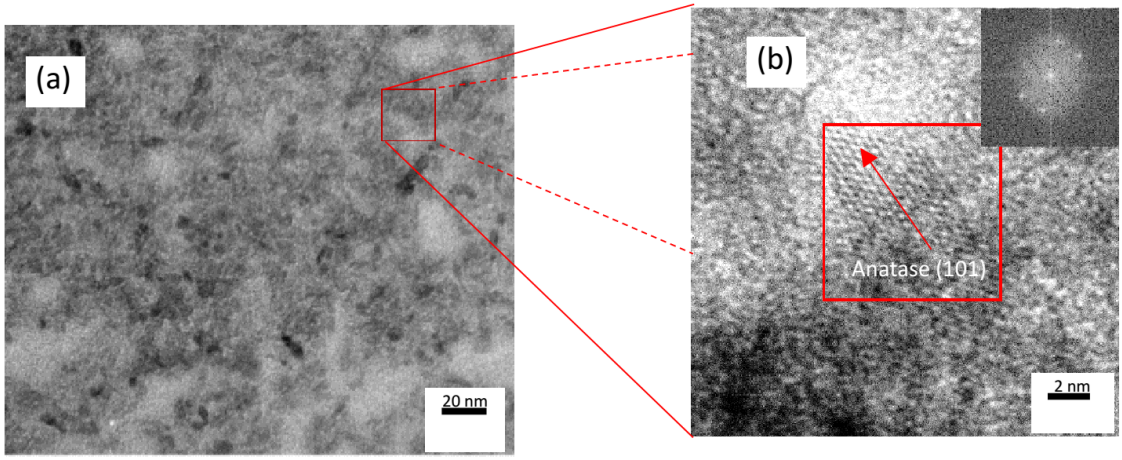

Fig. 2. (a) TEM and (b) HRTEM images of TiO_2 nanopaticles.

As can be seen from the TEM images in Fig. 2a, the TiO_2 in the suspension solution forms uniform grain-like clusters consisting of anatase particles with a mean size around 4-5 nm (Fig. 2b). This estimated size of TiO_2 nanoparticles is consistent to the mean size calculated from XRD.

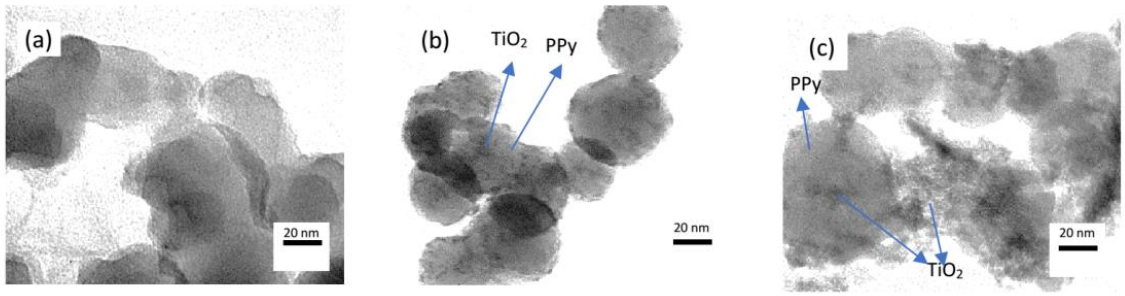

Fig. 3. TEM images of (a) neat PPy, (b) PPy/TiO_2 nanocomposite with 11% anatase TiO_2 and (c): PPy/TiO_2 nanocomposite with 33% anatase TiO_2

As expected, the strong coupling between PPy and TiO_2 can be seen from TEM images and Raman spectra made on PPy/TiO_2. TEM images show that the neat PPy has common structure of granular particle with mean size around 30-40 nm (Fig. 3a); and black TiO2 anatase nanoparticles with size around 3–4 nm randomly distributed on the surface and imbedded inside of PPy/TiO_2particles (Fig. 3b and Fig. 3c). Due to the difference in charge carriers density between TiO_2 (electron, insulator) and PPy (hole, semiconductor), the present of TiO_2 particle could

form a variety of carrier barriers or probably depletion junctions inside of PPy [25, 26], i.e., affecting the conductivity of the materials. In comparison to the core-shell structure of PPy/TiO_2 rutile [27] the random distribution of TiO_2 anatase nanoparticles in PPy matrix is expected to enhance the coupling effect between TiO_2 anatase and PPy.

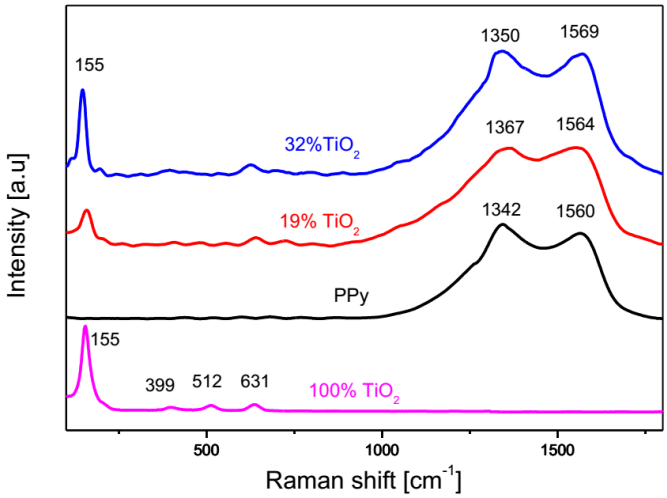

Fig. 4. Raman spectra of TiO_2, PPy and PPy/TiO_2 nanocomposite with different TiO_2 concentration.

As shown in Fig. 4 the Raman spectrum of neat PPy shows the instinct vibrational modes at 1560 cm^{-1} (G band) and 1342 cm^{-1} (D band). The presence of TiO_2 in the nanocomposite causes a change in relative intensity and a slight blue-shift of the vabration bands standing for C=C bond from 1342 cm^{-1} to 1350 cm^{-1} and 1560 cm^{-1} to 1569 cm^{-1} indicating a shift of PPy to the oxidation structure [22–24]. The higher oxidation degree of PPy is accounted for the strong coupling with TiO_2 anatase in the nanocomposites. From chemical view of consideration, at the first oxidization stage the TiO_2 surface in the reaction medium acts as nucleation sites for the Py radical monomers adsorbed and anchored on. As brought into contact with PPy, the higher oxidative anatase TiO2 will partly oxidize PPy and extract some electrons from PPy. Consequently, the conductance of p-type PPy and n-type TiO_2 will increase and variety of consecutive $p-n$ junctions are formed. The interfacial interaction between TiO_2 and PPy in the nanocomposites is expected to modify their chemical and electronic structures.

The effect of oxygen on the electrical conductivity of PPy and its derivatives is well known [28]. As an oxidized agent, the adsorbed oxygen molecule on the PPy surface abstracts a portion of electron from the pi-bond in the polymer chain and leave positive holes in the HUMO band of PPy, then converts the PPy to be a p-type semiconductor. The more adsorbed oxygen molecules are on the surface of PPy the higher the conductance of the materials is. Change the oxygen concentration in the ambient environment by changing the air pressure, the conductance of PPy will be modified. Experiments show that the resistance of PPy and PPy/TiO_2 is very sensitive to air pressure. As can be seen from the sensing profile in Fig. 5, the resistance of materials rapidly increases as air pressure reduces (the vacuum pump on) and fast recovers back to

the origin value as re-exposes to the air (the vacuum pump off). The presence of TiO_2 anatase in the PPy matrix significantly modifies the O_2 sensitivity of the materials. As can be seen from Fig. 5, the O_2 sensitivity of PPy/TiO_2 added with 11 at.% anatase TiO_2 exceeds 20 folds higher in comparison to that of neat PPy. This sensitivity is lightly higher than that of PPy coupling with TiO_2 rutile [27]. The fast response, recovery and the stability in base line from the O_2 sensing profile indicate the fact that the adsorption and desorption of oxygen molecules on PPy/TiO_2 surface is easy, namely the weak bonds (physical bonds) are dominant in the oxygen-PPy/TiO_2 interaction. Higher oxygen sensitivity indicates that more oxygen adsorption sites are created on the PPy/TiO_2 surface as anatase particles are incorporated.

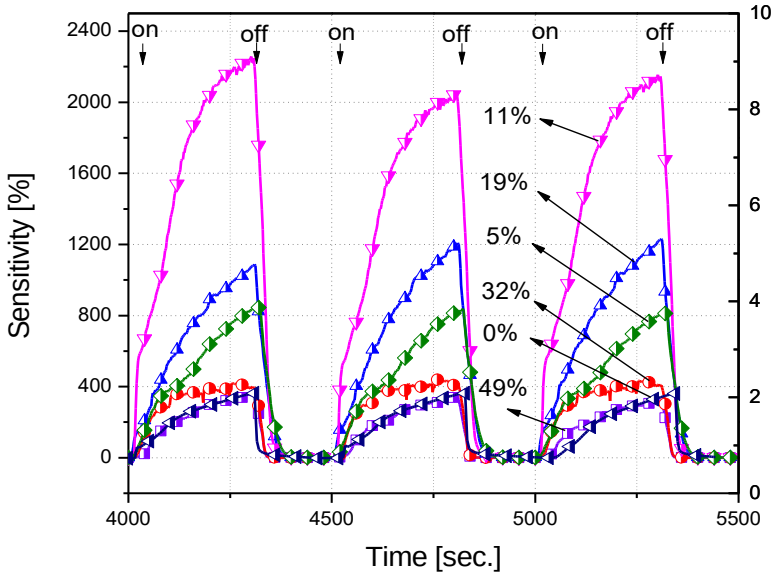

Fig. 5. The oxygen sensitivity profile of PPy/TiO_2 with different TiO_2 anatase concentration.

Table 1. Values of the impedance parameters in PPy/TiO_2 samples.

TiO_2 (at. %)	R_s (Ω)	C (F)	R_p (Ω)
0	330	3,11E-12	5,22E6
5	370	3,15E-12	1,69E6
11	340	2,74E-12	1,23E6
32	250	3,00E-12	4,23E6
49	270	2,97E-12	1,70E7

In order to explain the sensing and charge transport behavior of PPy and PPy/TiO_2 samples, a complex impedance spectroscopy is made. As shown in Fig. 6, a good agreement is observed between the experimental results (separated dots) and the simulated data (solid lines). the Nyquist plots of PPy and PPy/TiO_2 are perfect single semicircles. The semicircle plots can be fitted into a simple equivalent RC circuit which consists of a frequency independent resistance (R_s), a parallel

resistance R_p and a parallel capacitance C_p as in the inset. It has found that, parallel resistance R_p is very sensitive to the present of TiO_2 and air pressure, while the capacitance C_p and R_s are unchanged. Under the same air reduced pressure of - 0.6 bar the values of R_s, R_p, C_p obtained for PPy/TiO_2 samples with different TiO_2 contents are given in Table 1. As shown in Fig. 7, the R_p of PPy/TiO_2 nanocomposites is changed as a function of TiO_2 content. The PPy/TiO_2 nanocomposite added with 11 at.% anatase TiO_2 exhibits the lowest R_p, i.e., the highest conductance. The R_p then is assumed to be related to the formation of depletion layer between *n*-TiO_2 and *p*-PPy.

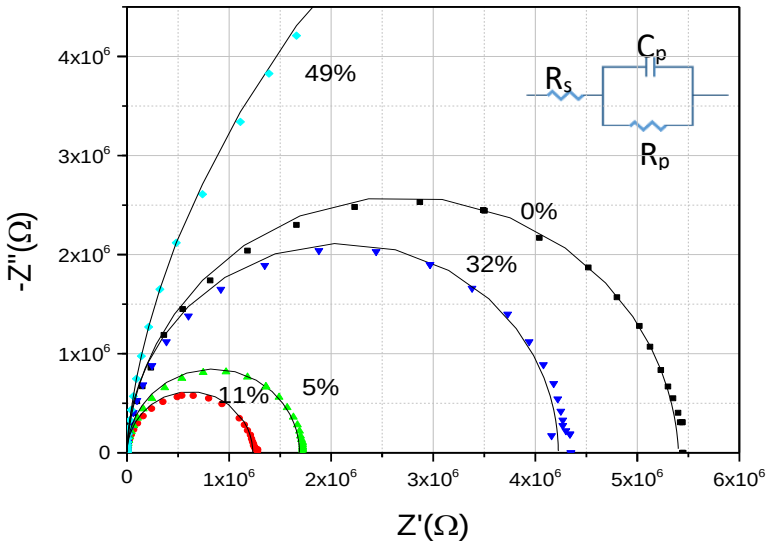

Fig. 6. Impedance spectra made on the PPy/TiO_2 nanocoposites with various TiO_2 anatase contents.

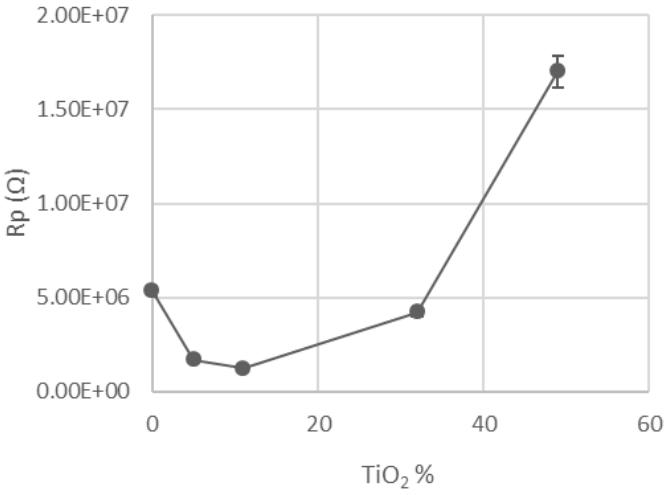

Fig. 7. The resistance Rp of PPy/TiO_2 as a function of TiO_2 concentration.

The Nyquist plots are shown in Fig. 8 and used to determine the effect of reduced air pressure on the charge transportation behavior of the PPy/TiO_2 sample with TiO_2 content of 11 at.%. As can be seen from the plots, the fitted spectrum is a semicircle with radius increasing with vacuum level. The semicircle gives the same equivalent circuit of R_s, R_p and C_p. The simulated results in Table 2 show that the R_s and C_p are almost unchanged but R_p is exponentially increased with reduced air pressure (Fig. 9).

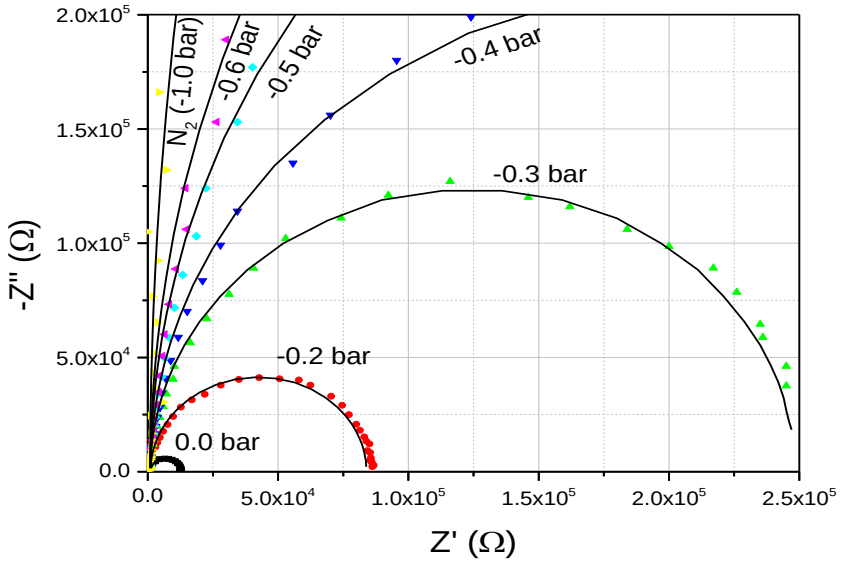

Fig. 8. Impedance spectra made on the PPy/TiO_2 nanocomposites in reduced air pressure and N_2 gas.

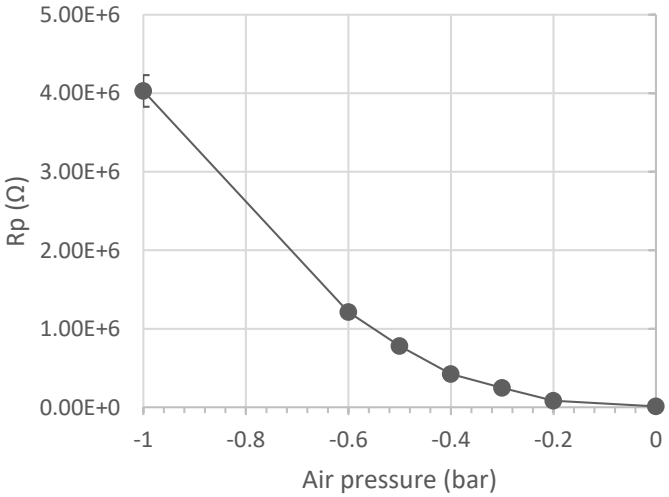

Fig. 9. The resistance Rp of PPy/TiO_2 as a function of reduced air pressure.

Table 2. Values of the impedance parameters in PPy/TiO_2 samples.

Air pressure [bar]	Rs (Ω)	Cp (F)	Rp (Ω)
0.0	1040	7.75E-12	11E+3
-0.2	1000	7.08E-12	83E+3
-0.3	980	6.61E-12	247E+3
-0.4	1020	6.68E-12	423E+3
-0.5	1050	6.67E-12	780E+3
-0.6	1060	6.60E-12	1,21E+6
N_2 environment	920	7.82E-12	4,03E+6

Based on the oxygen sensitivity, impedance spectra, it can be deduced that the sensing feature of PPy/TiO_2 is strongly affected by the surface states and interface layers ($p-n$ depletion region) between PPy and TiO_2. With anatase nanoparticles are randomly imbedded on the surface and inside of the PPy matrix, the PPy/TiO_2 structure will form a $n-p$ junction and depletion region depending on TiO_2 adding condition [25]. Upon exposure to the air, the charge exchange between oxygen and PPy/TiO_2 will form inversion regions of rich electron in a very thin layer near the $p-n$ PPy/TiO_2 contact and then modify the material conductance. Hence, the most sensitive R_p in the equivalent circuits R_s/C_pR_p is expected to be mainly associated with the material surface resistance. The modification of $n-p$ junction in the surface and inside of PPy/TiO_2 upon exposure to oxygen then is accounted for the oxygen sensitivity enhancement of the materials.

IV. CONCLUSIONS

PPy/TiO_2 nanocomposite synthesized by *in-situ* chemical polymerization shows that TiO_2 anatase nanoparticles with size around 3–4 nm are randomly embedded on the surface and inside of PPy grain. The PPy/TiO_2 coupling results in variety of carrier barriers on the surface and inside of PPy and then modify the PPy electronic properties. Upon exposure to oxygen (an oxidant and an electron acceptor) the charge exchange between oxygen and PPy/TiO_2 surface will form inversion layer in carrier barrier's contact region then modify the oxygen sensitivity of PPy. Upon exposure to reduced air pressure the conductivity of the nanocomposite exhibits a variation roughly about 20 folds that are accounted for the interaction between oxygen and the PPy surface. Complex impedance spectra show that the charge transport in the materials is equivalent to a circuit consisting of a frequency independent resistance (R_s) in series with RC network with capacitance C_p and resistance $R_p$in which the R_p is strongly sensitive to the environmental changing.

ACKNOWLEDGMENTS

This research is funded by the Hanoi University of Science and Technology (HUST) under project number T2016 - PC - 223.

REFERENCES

[1] Shirakawa, H., et al., .1. Shirakawa, H., et al., *Synthesis of Electrically Conducting Organic Polymers - Halogen Derivatives of Polyacetylene, (Ch)X.* Journal of the Chemical Society-Chemical Communications, 1977(16): p. 578-580.

[2] T. A Skotheim and J. Reynolds, *Handbook of Conducting Polymers, 2 Volume Set*. 2007: CRC press.

[3] R. A. Janssen *et al.*, *J. Chem. Phys.* **103** (1995) 788.
[4] T. K. Das and S. Prusty, *Polym. Plast. Technol. Eng.*, **51** (2012) 1487.
[5] A. F. Diaz and K. K. Kanazawa, *J. Chem. Soc., Chem. Comm.* **14** (1979) 635.
[6] M. Šetka, J. Drbohlavová and J. Hubálek, *Sensors* **17** (2017) 562.
[7] D. D. Ateh, H. A. Navsaria and P. Vadgama, *J. R. Soc. Interface* **3** (2006) 741.
[8] W. Sun and X. Chen, *J. Power Sources* **193** (2009) 924.
[9] L. Yongfang and Q. Renyuan, *J. Electroanal. Chem.* **362** (1993) 267.
[10] R. Gangopadhyay and A. De, *Chem. Mater.* **12** (2000) 608.
[11] A. Fujishima and K. Honda, *Letters to Nature* **238** (1972) 37.
[12] K. Hashimoto, H. Irie, and A. Fujishima, *Jpn. J. App. Phys.* **44** (2005) 8269.
[13] K. Nakata and A. Fujishima, *J. Photochem. Photobiol. C: Photochem. Rev.* **13** (2012) 169.
[14] M. M. Byranvand, *et al.*, *J. Nanostructures* **3** (2013) 1.
[15] D. N. Huyen, *et al.*, *Sensors (Basel)* **11** (2011) 1924.
[16] D. M. Lenz, M. Delamar and C. A. Ferreira, *J. Electroanal. Chem.* **540** (2003) 35.
[17] K. Jurewicz, *et al.*, *Chem. Phys. Lett.* **347** (2001) 36.
[18] Y. Gao *et al.*, *RSC Adv.* **4** (2014) 27130.
[19] N. T. Tung and D. N. Huyen, *Journal of Nanomaterials* 2016. **2016** (2016) 6547271.
[20] T. Tung Nguyen, X.D. Mai, and N.H. Duong, *Bull. Korean Chem. Soc.* **38** (2017) 401.
[21] G. Li *et al.*, *J. Am. Chem. Soc.* **130** (2008) 5402.
[22] S. J. Vigmond, V. Ghaemmaghami and M. Thompson, *Canadian J. Chem.* **73** (1995) 1711.
[23] Y. Furukawa *et al.*, *Synthetic Metals*, **24** (1988) 329.
[24] M. J. L. Santos, A. G. Brolo and E. M. Girotto, *Electrochim. Acta* **52** (2007) 6141.
[25] O. Inganäs, T. Skotheim and I. Lundström, *J. App. Phys.* **54** (1983) 3636.
[26] P. S. Abthagir and R. Saraswathi, **81** (2001) 2127.
[27] N. T. Tung, and D. N. Huyen, *J. Nanomater.* 2016. **2016** 4283696.
[28] X. Li, R. Ramasamy and P.K. Dutta, *Sensors and Actuators B: Chemical* **143** (2009) 308.